Isolation of Zn and Cr in Biosolid Waste by Extraction Process Using Sulfuric Acid

by

3rd International Conference Eco-Innovation in Science, Engineering, and Technology
Volume 2022
http://dx.doi.org/10.11594/nstp.2022.2720

Conference Paper

Crystallization of Barium Sulfate with Magnesium Chlorite and Calcium Chlorite Additives

Novel Karaman[1]*, Susilowati[1], Gerri Adhit Fachriansyah[2], Reffi Allifyanto[2], A. P. Bayuseno[3]

[1]Master of Environmental Science, Engineering Faculty, Universitas Pembangunan Nasional "Veteran" Jawa Timur, Surabaya 60294, Indonesia
[2]Chemical Engineering Program, Engineering Faculty, Universitas Pembangunan Nasional "Veteran" Jawa Timur, Surabaya 60294, Indonesia
[3]Department of Mechanical Engineering, Diponegoro University, Semarang, Indonesia

*Corresponding author:
E-mail:
novel_karaman05@yahoo.com

ABSTRACT

Barium sulfate scale grew on industrial oil equipment make damaged either in injection or producing wells. A series of experiments were performed to estimate the precipitation rate of barium sulfate in laboratory equipment from brines containing the concentration of barium ions (3500 ppm) and varying concentrations of calcium and magnesium ions (10 and 20 ppm). Additionally, stirring speeds (240 and 480 rpm) affecting the crystallization of barium sulfate scales were also studied through kinetic analysis. At a certain stirring speed, the precipitation of the barium sulfate scale decreased since its solubility increased with increasing concentrations of Ca and Mg-cations, as indicated by changes in constant rate values. All solid crystals obtained from experiments contained mainly pure barite as validated by X-Ray Diffraction (XRD) method. The SEM micrograph for the morphology of barite showed particles with prismatic and tabular-shaped crystals on the order of 2 to 5 µm particles. The kinetic results provided a general reaction rate equation that can predict barium sulfate deposition in the reservoir for a given brine, supersaturation, and time durations of mixing.

Keywords: Barium Sulfate, Ca and Mg cations stirring speed, SEM, XRD

Introduction

A mineral-scale deposit of barium sulfate (BaSO4) may be commonly found in petroleum industries due to incompatibility between the injection water and the reservoir water and crude oil (BinMerdhah et al., 2010; Jones et al., 2005; Liu, 2022). In contrast, water contains major salts (i.e., sodium chloride) and varying amounts of calcium salt, potassium, magnesium, carbonates, bicarbonates, and chlorides. These chemical compounds present in the injection water influence barium sulfate scale formation in the reservoir. Major factors controlling growing barium sulfate scale deposits include temperature, pressure, ion strength, evaporation, contact time, and pH. Specifically, barium sulfate easily accumulates in oil wells due to its highly insoluble substance (solubility is only 2 mg/liter in water). Solubility in the barium sulfate scale increases with temperature, inversely proportional to the calcium carbonate scale. The solubility of barium sulfate is lower than that of calcium carbonate. Unlike calcium sulfate and carbonate scales, the barium sulfate scale is very compact with high hardness, making it not easy to remove, even using the acid treatment (Mhatre et al., 2021).

In particular, the crystallization of barium sulfate could be modeled in a simple system by elucidating factors controlling crystallization processes, including the functional group (Charlesa et al., 2022), lattice matching (Jones et al., 2006), and charge effects (Jones et al., 2001).

How to cite:
Karaman, N., Susilowati, Fachriansyah, G. A., Allifyanto, R., & Bayuseno, A. P. (2022). Crystallization of barium sulfate with magnesium chlorite and calcium chlorite additives. *3rd International Conference Eco-Innovation in Science, Engineering, and Technology*. NST Proceedings. pages 120-130. doi: 10.11594/ nstp.2022.2720

Specifically, previous studies examine the effects of aspartic acid organic and inorganic presence (Akyol et al., 2016) and the alkali metals (Li et al., 2021; Jones et al., 2004; Jones et al., 2018; Widanagamage et al., 2018) on barium sulfate crystallization. In the mode of crystallization, it was reported that the barium ion is partially de-solvated in the solution in the presence of aspartic acid, which is subsequently incorporated into the barium lattice structure. The result suggested that knowledge of barium ion desolvation became necessary for rate-determining barium sulfate crystallization (Widanagamage et al., 2015; Kowacz et al., 2007; Shikazono, 1994; Boon & Jones, 2016).

Instead, the previous study on favorable crystallization of barium ions (i.e., $Ba2+/SO42- > 1$) by AFM (atomic force microscopy) method proposed the non-stoichiometric composition yielded faster crystal growth rates on (0 0 1) lattice face (Judat & Kind, 2004; Kuwahara et al., 2016). However, only limited research work has investigated the impact of inorganic anions (Ca2+ and/or Mg2+) on barium sulfate crystallization, while most studies focused on determining the solid solution formation (Wong et al., 2001; Widanagamage et al., 2014). In addition to the inorganic anion and halogens ((Wong et al., 2001; Widanagamage et al., 2014; Appleo & Postma, 2005; Hennessy & Graham, 2002; Smith et al., 2004; Barouda et al., 2007), carbonate ($CO32-$) was suggested to render barium sulfate crystallization (Appleo & Postma, 2005; Hennessy & Graham, 2002; Smith et al., 2004; Barouda et al., 2007; Aboelezz et al., 2021; Jones et al., 2018). Therefore, the different behavior of barium sulfate crystallization may occur in the solution containing magnesium, sodium, and calcium through both stereochemistry (lattice matching) and/or ionization mechanisms (Aboelezz et al., 2022; Qasim & Mousa, 2021; Freeman et al., 2006; Judat & Kind, 2004).

Despite much work examining various organics and inorganics for influencing barium sulfate crystallization, fundamental questions remain to be quest to predict their impacts on scale formation in a simple laboratory system, regardless of promotion or inhibition consideration (Shaw et al., 2012; Sadeghalvad et al., 2021). The study's purpose was to investigate the effects of calcium or magnesium cations present in the synthetic brines on the precipitation of barium sulfate. Specifically, the influences of calcium or magnesium concentrations and stirring rates on morphology and deposition rates were evaluated. Mineralogy and morphology alteration from the aqueous crystallization system was examined by XRPD (X-ray powder diffraction) and SEM (scanning electron microscopy) analysis. This crystallization experiment predicts a general trend of barium sulfate crystallization in the water reservoir.

Material and Methods

Crystal forming solution

Analytical grade powders $BaCl2.2H2O$, $Na2SO4$, $CaCl2$, and $MgCl2$ (Merck Germany) were prepared in a given weight dissolved in distilled water that was used throughout the present study, and barium sulfate was synthesized according to the following reaction (Eq.1);

$$BaCl2\ (aqueous) + Na2SO4\ (aqueous) \rightarrow BaSO4\ (salt) + 2NaCl\ (aqueous)$$

In each experiment, 31.165 g $BaCl2.2H2O$ solid and 18.1 g $Na2SO4$ were dissolved in 5 L water so that 3500 ppm of barium and sulfate concentrations were obtained for the synthetic form of brine. The brines' pH values were allowed to change naturally because the barium sulfate crystallization was unresponsive to the pH values (3-9). Subsequently, brines 1 and 2 were set up for each experiment with varying concentrations of calcium or magnesium. Correspondingly, $MgCl2$ solids (0.195 g and 0.39 g) were dissolved in 1000 ml of water to provide solution concentrations of 10 ppm and 20 ppm. Similarly, 0.135 g and 0.275 g $CaCl2$ were suspended in 1000 ml water to prepare 10 and 20 ppm solution concentrations. The stirring rates for mixing brine were set for 240 and 480 rpm.

Crystallization experiments

Two glass burettes were used to deliver known volumes of brines containing barium and sulfate into a glass flask of 1000 ml capacity. Each solution of barium and sulfate ions with 100 ml volume was dropped from each burette into the flask. Later, the stirring temperature of 30 ^{O}C and stirring speed (240 and 480 rpm) were set accordingly. Afterward, the magnetic stirrer was switched-on, and the mixing of the brine-rich solution was started, while for each experiment, the mass of the barium crystal product was taken every 30 minutes for kinetic analyses and ended at 120 min. In the case of the experiment for brines and 2, (BS1-Ca) and (BS2-Mg), Ca or Mg-concentrations were added separately into the mixture of the solution. Herewith BS1-Ca0, BS1-Ca10, and BS1-Ca20 are presented as samples formed from barium sulfate with Ca-cations of 0, 10, and 20 ppm, respectively. Similarly, BS2-Mg0, BS2-Mg10, and BS2-Mg20 are samples formed from barium sulfate with Mg-cations of 0, 10, and 20 ppm, respectively. At the end of the experiments, all barium sulfate scales were strained by a 0.45-µm paper filter. Later, drying the obtained solid scales was performed in the oven at 100 ^{O}C for 24 h and subsequently weighed for deposition mass rate assessment. Instead, scale samples from each experiment were taken for XRD and SEM analysis to observe the crystal and morphological structures of the scales.

Powder samples characterization

All precipitated samples were subjected to the XRD (x-ray diffraction) method for mineralogy analysis, by which data were collected by the X-ray diffractometer (Bragg Brentano mode- Philips; PW 3050/60). In this measurement, parameters of Cu-Kα radiation (l=1.5406 Å) were set-up for 10-60O 2q scans, 0.02O steps, and 0.5 s/step. The phase identification of the minerals scale was performed by the search-match program of QualX (Altomare et al., 2008). Later, XRD Rietveld analysis (Program Fullprof-2k, version 3.30) performed the verification of previously identified phases (Rodriguez-Carvajal, 2005). For running the XRD, Rietveld refinements employed the crystal structure model available COD (Crystallography Open Database) (Mahieux et al., 2010). The XRD Rietveld refinement strategy discussion is presented elsewhere (Grazulis et al., 2009). On the other hand, the SEM/EDX (JEOL JSM 5200) method was used for morphology analysis of micrographs obtained from 20.0 kV and 1.0 nA experimental conditions. Before the investigation, the examined powders placed by gluing on the surface of the metallic sample holder were then coated with gold.

Results and Discussion

Isolation of Actinomycetes from termite's nest sample

Kinetics of barium sulfate precipitation varying stirring rates were analyzed based on a first-order reaction according to the following (Eq. 2);

$$A \rightarrow \text{products} \qquad (2)$$

If the infinitesimal changes in concentration and time are considered, then the kinetic rate equation can be written as:

$$\text{Rate}(\text{Ms}^{-1}) = -\frac{d[A]}{dt} = k[A] \qquad (3)$$

By integrating the form of the reaction provides the reaction equation simply expressed as

$$\int_{[A]o}^{[A]} \frac{d[A]}{[A]} = -k\int_{0}^{t} dt \qquad (4)$$

$$ln\frac{[A]}{[A]o} = -k * t \quad (5)$$

Here, [A]O represents the initial concentration of species at time, t = 0, while [A] = [A] at time = t. Using this reaction equation takes a plot of k*t versus [A] in a straight line for determining the kinetics of reaction for $BaSO_4$ precipitation according to

$$Ba^{2+} + SO_4^{2-} \rightarrow BaSO_4 \quad (6)$$

Where molar concentrations of [A] represents [Ba^{2+}].

In each experiment for kinetic analysis, a solution concentration of Ba^{2+} (3500 ppm) and additives of Ca and Mg-ions in the amounts of 0, 10, and 20 ppm were investigated for varying stirring speeds (240 and 480 rpm). The experimental results elucidated the expected trend of $BaSO_4$ precipitation with increasing time durations and stirring speed (Figure 2). Hence, the crystallization kinetics of brines were estimated as either the rate of reduction of Ba^{2+} or the increment rate of time. Correspondingly, the barium concentration [Ba^{2+}] precipitated from the solution can be linked to the observed stirring speed values and time duration, as reported in Eq. (6). In the absence and presence of Ca^{2+} and Mg^{2+}, a reduction in the Ba^{2+}-concentration could be observed during the experiment run. Accordingly, the change in the Ba^{2+}-concentration in 0-120 minutes was after the $BaSO_4$ formation.

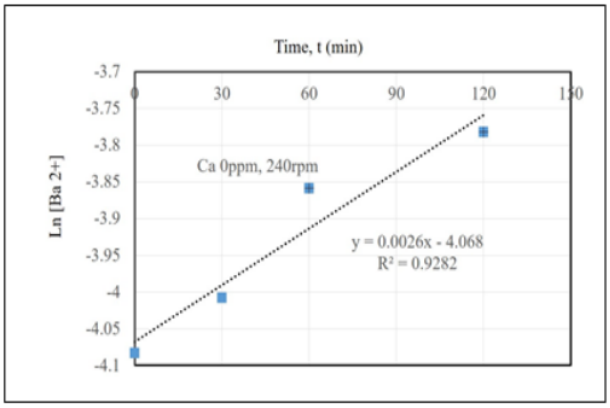

Figure 1. First-order kinetic of barium sulfate crystallization (BS0-sample) in 0-120 min in the absence of Ca-ion and stirring speed of 240 rpm

Further kinetic analysis of the BS0-sample provided the line of best fit for the typical data in the absence of Ca- ions. For first-order kinetics, a correlation coefficient (R^2) of 0.9282 could be reliable in determining the precipitation rate of a barium sulfate crystal. Additionally, other kinetic forms for brines (BS-Ca and BS-Mg) followed the crystallization first-order reaction rates. The adsorption rate constants (k) of BS-Ca samples could be explored from the slopes of the straight lines as presented in Table 1. The experiment runs at 240 rpm and in the absence of Ca-ions, provides the calculated reaction rate value of 2.6 x 10^{-3} M min^{-1}, which agreed very well with reported data in which the order values of 5 x 10^{-3} and 2 x 10^{-2} are commonly followed by the barium sulfate crystallization (BinMerdhah et al., 2010).

Moreover, the rate constant of barium sulfate precipitation from the solution increased slightly at a stirring speed of 480 rpm. Moreover, the effect of Ca-ions on the mass precipitation of barium sulfate could be inferred from the obtained reaction rate constants. Apparently, the reaction rate constant decreased as the Ca-ion concentration increased. The above data suggested that the greater concentration of Ca-ions may inhibit the growth of barium sulfate crystals, whereby the increasing stirring speed accelerated the rate of growth/formation of barium sulfate crystals. Instead, the presence of calcium reduced the nucleation rate of scale formation. Additionally, the presence of Ca-cation may increase the solubility of barium sulfate, mainly at very high supersaturation (Hennessy & Graham, 2002).

Likewise, the relationship between the effect of Mg-ion and stirring speed (rpm) and the crystallization product of barium sulfate crystals could be estimated by the first-order reaction kinetics (Table 2), while the calculated rates did agree with the previously reported data (BinMerdhah et al., 2010). The reaction rates of the barium sulfate products reduced slightly Mg-ion concentration but increased with higher stirring speeds. Compared with similar Ca-effect results, Mg^{2+} "destroys" inhibited barium sulfate precipitation (Shaw et al., 2012).

Table 1. Varying reaction rate constants for barite crystallization in the presence of Ca^{2+}

Ca^{2+} (ppm)	Mass (mg)	Stirring speed (rpm)	Regression equation	Rate constant (k, M min^{-1})	R^2
0	0.0312	240	y = 0.0026x - 4.068	2.6 x 10^{-3}	0.9282
0	0.0367	480	y = 0.0037x - 4.0215	3.7 x 10^{-3}	0.9307
10	0.0421	240	y = 0.0017x - 3.6769	1.7 x 10^{-3}	0.9201
10	0.0455	480	y = 0.0016x - 3.5943	1.6 x 10^{-3}	0.9759
20	0.0488	240	y = 0.0022x - 3.5828	2.2 x 10^{-3}	0.9400
20	0.0494	480	y = 0.0016x - 3.4808	1.6 x 10^{-3}	0.9703

Table 2. Varying reaction rate constants for barite crystallization in the presence of Mg^{2+}

Mg^{2+} (ppm)	Mass (mg)	Stirring speed (rpm)	Regression equation	Rate constant (k, M min^{-1})	R^2
0	0.0312	240	y = 0.0026x - 4.068	2.6 x 10^{-3}	0.9282
0	0.0367	480	y = 0.0037x - 4.0215	3.7 x 10^{-3}	0.9307
10	0.0467	240	y = 0.0022x - 3.6294	2.2 x 10^{-3}	0.9504
10	0.0531	480	y = 0.0015x - 3.4254	1.5 x 10^{-3}	0.9043
20	0.0553	240	y = 0.0008x - 3.2909	0.8 x 10^{-3}	0.9031
20	0.0621	480	y = 0.0013x - 3.2411	1.3 x 10^{-3}	0.9744

Purity of the crystal products

The crystallized barium sulfates from the solution in the absence and presence of Ca and Mg (0, 10, and 20 ppm) were validated qualitatively by the XRD method based on computerized search-match procedures. The phase identification of all measured XRD data confirmed the single phase of barium sulfate (barite) crystallized at the stirring speeds (240 and 480 rpm) according to the (Crystallography Open Database) COD card number# 9014889. Subsequently, the XRD-Rietveld method refined these crystal structure data (Antao, 2012), providing the best refinement plot between observed and calculated data, as shown for the BS0-sample in Figure 2a. Correspondingly, the present study obtained the single-phase barite, regardless of varying concentrations of Ca-cations and stirring speeds. In particular, no additional peaks could be identified for other samples (Figure 2b). The composition of the collected precipitate phases was not modified

under the influence of these Ca^{2+} concentrations. As a result of the minerals forming a solid solution, precipitates may consist of a mixture of any single crystal.

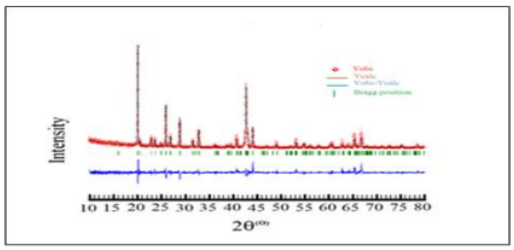

Figure 2a. XRD Rietveld analysis of BS0-sample

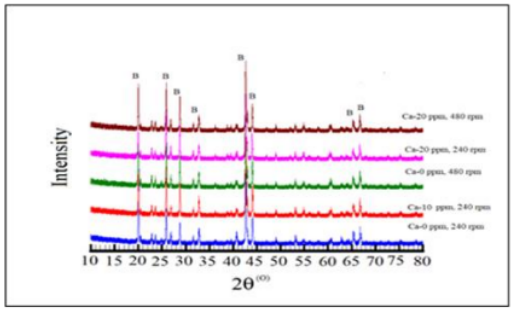

Figure 2b. X-ray diffractograms of barium sulfate (B) crystals precipitated in the absence and presence of Ca-ions

Instead, BS2-Mg0, BS2-Mg10, and BS2-Mg20 specimens containing pure barite could be validated by Rietveld refinements of the XRD data given in Figure 2c. Barite crystals could be synthesized with crystal structure data agreeing with those of the reported study [38]. Further examination of XRD data for all specimens was confirmed by the similarity in the crystal structure of barite with increasing magnesium (10 and 20 ppm) and stirring speeds (240 and 480 rpm).

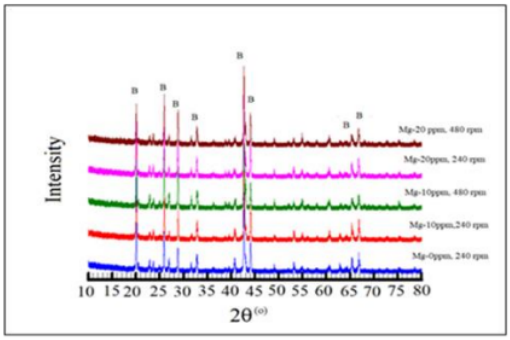

Figure 2c. X-ray diffractograms of barium sulfate (B) crystals precipitated in the absence and presence of Mg-ions

Morphology character of the synthesized barite

Effects of varying concentrations of calcium and magnesium and constant stirring speeds of 240 and 480 rpm on morphology were examined on SEM micrographs. Figure 3 shows the morphologies of the resultant barite crystals in the presence of calcium. Generally, the shape and crystal growth of barite observed during the present study are similar to those of natural barite crystals. Regardless of the presence of Ca-cations, prismatic or tabular-shaped crystals on the order of 2 to 5 microns could be observed because they were grown under normal conditions. This indicates that deposition conditions on the surface of the down-hole in the oil production field may insignificantly control the morphology of the barite product (Lopresti et al., 2021; Turner & Filella, 2021).

The morphology of the obtained barite for the BS0 sample has prismatic platelets with some overgrowth on the base plates, which results in pyramidal growth (Figure 3a). There is also a small shape of tabular formed, but some crystals changed into all rectangular platelets with an increasing stirring speed of 480 rpm (Figure 3b). With further increasing calcium levels (10 ppm), the crystals lose their preferential growth directions and become more compact (Figure 3c). At Ca of 20 ppm stirred at 240 rpm, the platelets still have sharp edges, whereas stirred at the edges are irregular, and the particles appear scaly (Figure 3d). When stirred at 480 rpm, the particles have completely lost their plate-like shape and become pyramidal (Figure 3e).

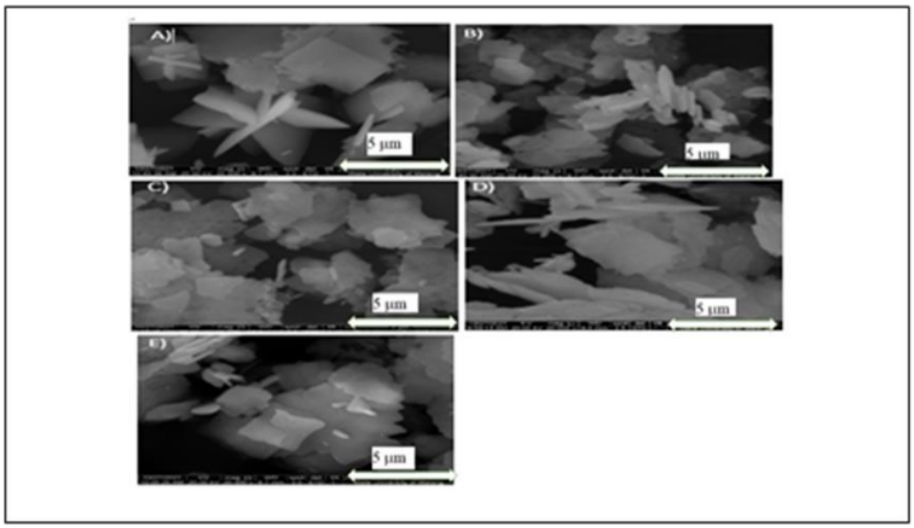

Figure 3. SEM Micrographs of barium sulfate crystals in the presence of Ca ions for samples; a) BS0, 240 rpm; b) BS1-Ca10, 240 rpm; c) BS1-Ca10, 480 rpm; d) BS1-Ca20, 240 rpm; e) BS1-Ca20, 480 rpm

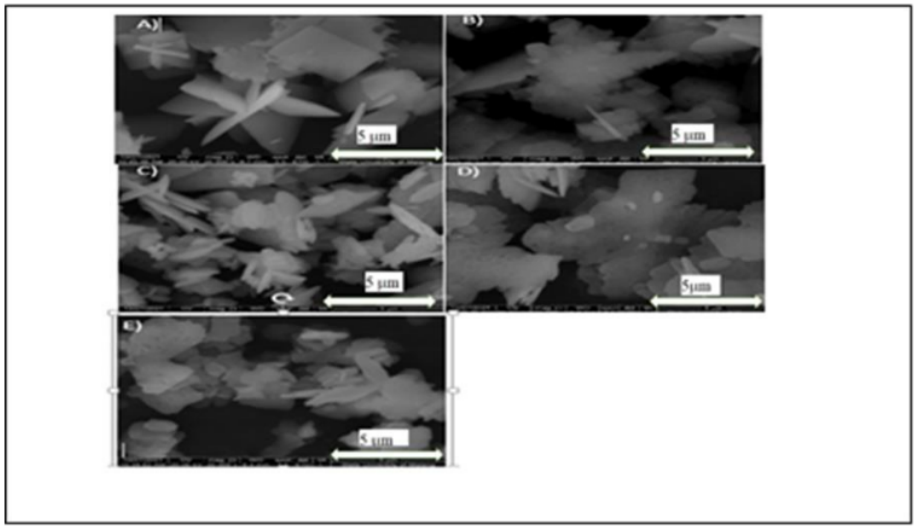

Figure 4. SEM Micrographs of barium sulfate crystals in the presence of Ca ions for samples; a) BS0, 240 rpm; b) BS1-Ca10, 240 rpm; c) BS1-Ca10, 480 rpm; d) BS1-Ca20, 240 rpm; e) BS1-Ca20, 480 rpm

In contrast, the morphologies of the barium sulfate crystal in the free magnesium concentration are shown in Figure 4. The magnesium levels were added in amounts of 10 and 20 ppm, providing the similarity in the morphologies of barium sulfate with particle sizes less than 5 µm. The notable differences could then be observed in only a sample of BS2-Mg10 stirred at 480 rpm showing various growth forms of barium sulfate (Figure 4c). However, all particles seemed to change to make pyramidal particles all more condensed particles (Figures 4d and e). These morphology results suggested that agglomeration had occurred in all samples observed in the present work. Strong, attractive interactions between those faces made particle aggregation under changed stirring speed possible. Thus, the aggregation of crystallites may play a role in the submicrometer size for self-assembled particles (Lopresti et al., 2021; Turner & Filella, 2021).

Implications of the present work

The simple laboratory system demonstrated the effects of calcium and magnesium present in synthetic brine on the kinetics and morphology of barite crystallization. The presence of those divalent ions of [Ca^{2+}] and [Mg^{2+}] may increase the solubility of barium sulfate, along with the lower supersaturation. The ionic strength and ion-pair formation at higher concentrations for [Ca^{2+}] and [Mg^{2+}] have been suggested to contribute to the increased solubility of barite (Bin-Merdhah et al., 2010). Specifically, calcium may incorporate into barite lattices of up to 17 %, increasing solubility. Consequently, ion incorporation caused the order of magnitude changes in solubility observed here with the reduced mass of the precipitating solid. However, the calcium and magnesium concentrations employed in the study were up to 20 ppm, which was still below the significant concentration of 1.25 mM for ion-pairing formation reported in the literature ((Bin-Merdhah et al., 2010; Hennessy & Graham, 2002). Further possible increases in the solubility of barium sulfate in these solutions may be expected from purely ionic strength considerations. Accordingly, mechanisms for reduced mass precipitation may be from absorbing calcium and magnesium ions onto the barium sulfate surface, hindering further barium sulfate precipitation (surface poisoning).

Generally, calcium present in the brines solution may inhibit barium sulfate precipitation, whereas the presence of magnesium tends to reduce its inhibition efficiency (Hennessy & Graham, 2002). It has been demonstrated in the study that the effect of calcium and magnesium cations could be inferred from the estimated values of reaction rates (Tables 1 and 2). Furthermore, the presence of divalent cations [Ca^{2+}] and [Mg^{2+}] caused the reduction of the precipitated mass of barium sulfate crystals, which could be related to the lower supersaturation and higher solubility of barium sulfate. Barium sulfate saturation ratio (SR) according to (Eq.7);

$$SR = \frac{\left[Ba^{2+}\right]\left[SO_4^{2-}\right]}{K_{sp}} \quad (7)$$

Where [Ba^{2+}] is initial barium-ion concentration (mol/l); [SO_4^{2-}] is initial sulfate-ion concentration (mol/l); and Ksp is barium sulfate solubility product, at temperature T, specific pH, and ionic-strength level and Ksp for barium sulfate at 30 ^{o}C is 1.2 x 10^{-10} mol^2 L^{-2}. In the present experiment, SR represented the degree of supersaturation and was computed using an initial barium concentration of 3500 ppm, providing an SR of 775.69. The barite SR remained constant during experiments, whereas only [Ca^{2+}] and [Mg^{2+}] concentrations were changed. Accordingly, any inhibition or promotion of nucleation or precipitation of barium sulfate particles in the presence of calcium and magnesium could not be concluded from the present experiment. Further research should be done on the synthesis of barium sulfate with varying temperatures, ratios of [Ca^{2+}] and [Mg^{2+}], and pH of the brine mix for the longer reaction time. Our new sequential synthesis protocol permits the design of a reactor to produce barium sulfates in need of many industrial sectors such as building and health industries (Kou et al., 2021; Kumar et al., 2021; Gomaaa et al., 2021; Caltran et al., 2021).

Conclusion

Divalent cations (Ca2+ and Mg2+) and stirring speeds influencing barium sulfate scale precipitation have been examined. The experimental results demonstrated that with the decrease of mass precipitation of barium sulfate in the presence of calcium and magnesium, pure barite was generated in the synthetic brine experimental conditions. In addition, no change in the phase composition of barite with the presence of calcium and magnesium and stirring speeds was evident. The morphology of barite has been proven on SEM micrographs showing mainly pyramidal-shaped crystals and fewer crystals with tubular shapes. In particular, a general reaction rate equation for barium sulfate precipitation from the reservoir for a given brine, supersaturation, and time durations of mixing could be determined.

References

Aboelezz, E., Bortolin, E., Quattrini, M. C., & Monaca, S. D. (2022). TL and OSL studies on irradiated nano barium strontium sulfate to photons, electrons and protons. *J. Lumin, 242,* 118592. https://doi.org/10.1016/j.jlumin.2021.118592.

Aboelezz, E., De Angelis, C., & Fattibene, P. (2021). A study on energy dependence of nano barium sulfate powder using the EPR technique in photon, electron and proton beams. *Measurement, 175,* 109108. https://doi.org/10.1016/j.measurement.2021.109108

Akyol, E., Aras, O., & Oner, M. (2016). Control of barium sulfate crystallization in the presence of additives, desalin. *Water, 52,* 5965-5973. https://doi.org/10.1080/19443994.2013.808589

Altomare, A., Cuocci, C., Giacovazzo, C., Moliternia, A., & Rizzia, R. (2008). QUALX: a computer program for qualitative analysis using powder diffraction data. *J. Appl. Cryst., 41,* 815-817. https://doi.org/10.1107/S0021889808016956

Antao, S. M. (2012). Structural trends for celestite (SrSO4), anglesite (PbSO4), and barite (BaSO4): confirmation of expected variations within SO4 groups. *Am. Mineral., 97,* 661–665. https://doi.org/10.2138/am.2012.3905

Appleo C. A. J., & Postma, D. (2005). *Geochemistry, Groundwater and pollution*. 2nd ed., CRC Press: Boca Raton, FL, USA, 152–154.

Barouda, E., Demadis, K. D., Freeman, S. R., Jones, F., & Ogden, M. I. (2007). Barium Sulfate Crystallization in the presence of variable chain length aminomethylenetetraphosphonates and cations (Na+ or Zn2+). *Cryst. Growth Des., 7,* 321-327. https://doi.org/10.1021/cg0604172

BinMerdhah, A. B., Yassin, A. A. M., & Muherei, M. A. (2010). Laboratory and prediction of barium sulfate scaling at high-barium formation water. *J. Pet. Sci. Eng., 70,* 79-88. https://doi.org/10.1016/j.petrol.2009.10.001.

Boon, M., & Jones, F. (2016). Barium sulfate crystallization from synthetic seawater. *J. Cryst. Growth, 16*, 4646. https://doi.org/10.1021/acs.cgd.6b00729

Caltran, I., Kukuh, F. A., Rietveld, L. C., Gerard, S., & Heijman, J. (2021). Sulfate precipitation treatment for NOM-rich ion exchange brines. *Sep. Purif. Technol., 269*, 118669. https://doi.org/10.1016/j.seppur.2021.118669.

Carmona-Quiroga, P. M., & Blanco-Varela, M. T. (2021). Barium carbonate and supplementary cementitious materials to counteract thaumasite sulfate attack in mortars: Effect of aggregate composition. *Constr Build Mater, 282*, 122583. https://doi.org/10.1016/j.conbuildmat.2021.122583.

Charlesa, S., Buia, D. W., Canlera, T., & Carnevali, A. (2022). Strontium in barium sulphate as a discriminating factor in the forensic analysis of tool paint by SEM/EDS. *Forensic Sci. Int., 331*, 111127. https://doi.org/10.1016/j.forsciint.2021.111127

Jones, F., Oliviera, A., Parkinson, G. M., Rohl, A. L., Stanley, A., & Upson, T. (2004). The effect of calcium ions on the precipitation of barium sulphate 1: calcium ions in the absence of organic additives. *J. Cryst. Growth, 262*, 572–580. https://doi.org/10.1016/j.jcrysgro.2003.10.069

Freeman, S. R., Jones, F., Ogden, A. O., & Richmand, W. R. (2006). Effect of benzoic acids on barite and calcite precipitation. *Cryst. Growth Des., 6*, 2579. https://doi.org/10.1021/cg060186z

Gomaaa, H. E., Alotaibi, A. A., Gomaac, F. A., Bajuayfir, E., Ahmad, A., & Alotaibi, K. M. (2021). Integrated ion exchange-based system for nitrate and sulfate removal from water of different matrices: Analysis and optimization using response surface methodology and Taguchi experimental design techniques. *Process Saf. Environ. Prot., 153*, 500-517. https://doi.org/10.1016/j.psep.2021.07.045.

Grazulis, S., Chateigner, D., Downs, R. T., Yokochi, A. F. T., Quiros, M., Lutterotti, L., Manakova, E., Butkus, J., Moeck, P., & Le Bail, A. (2009). Crystallography open database - an open-access. *J. Appl. Cryst., 42*, 1-4. https://doi.org/10.1107/S0021889809016690

Hennessy, A. J. B., & Graham, G. M. (2002). The effect of additives on the co-crystallization of calcium with barium sulphate. *J. Cryst. Growth, 237–239,* 2153-2159. https://doi.org/10.1016/S0022-0248(01)02258-8

Jones, F., Clegg, J., Oliviera, A., Rohl, A.L., Ogden, M. I., Parkinson, G. M., Fogg, A. M., & Reyhani, M. M. (2001). The effect of phosphonate-based growth modifiers on the morphology of hematite nanoparticles formed via acid hydrolysis of ferric chloride solutions. *CrystEngComm., 40,* 1-3. https://doi.org/10.1039/B201288J.

Jones, F., Ogden, M. I., & Radomirovic, T. (2018). The impact of oxalate ions on barium sulfate crystallization. J. Cryst. Growth 2018, 498, 148-153. https://doi.org/10.1016/j.jcrysgro.2018.06.014

Jones, F., Ogden, M. I., & Radomirovic, T. (2018). The impact of oxalate ions on barium sulfate crystallization. *J. Cryst. Growth, 498*, 148-153. https://doi.org/10.1016/j.jcrysgro.2018.06.014

Jones, F., Richmond, W.R., & Rohl, A. L. (2006). Molecular modeling of phosphonate molecules onto barium sulfate terraced surfaces. *J. Phys. Chem. B., 110*, 7414–7424. https://doi.org/10.1021/jp054916.

Jones., F., Mocerino, M., Ogden, M. I., Oliviera, A., & Parkinson, G. M. (2005). Bio-Inspired Calix[4]arene additives for crystal growth modification of inorganic materials. *Cryst. Growth Design, 5,* 2336–2343. https://doi.org/10.1021/cg050322k

Judat, B., & Kind, M. (2004). Morphology and internal structure of barium sulphate-Derivation of a new growth mechanism. *J. Colloid Interface Sci., 269*, 341. https://doi.org/10.1016/j.jcis.2003.07.047

Judat, B., & Kind, M. (2004). Morphology and internal structure of barium sulfate—derivation of a new growth mechanism. *J. Colloid. Interface Sci., 269,* 341-353. https://doi.org/10.1016/j.jcis.2003.07.047

Kou, Y., Wang, Y., Zhang, J., Guo, K., Zhang, X., Yu, Z. H., & Song, X. (2021). Nano BaSO4 prepared by microreactor and its effect on thermal decomposition of some energetics. *FirePhysChem, 2,* 174-184. https://doi.org/10.1016/j.fpc.2021.11.004

Kowacz, M., Putnis, C. V., & Putnis, A. (2007). The effect of cation:anion ratio in solution on the mechanism of Barite growth at constant supersaturation: Role of desolvation on the growth kinetics. Geochim. Cosmochim. *Acta, 71,* 5168 https://doi.org/10.1016/j.gca.2007.09.008

Kumar, N., Grewal, J. S., Kumar, S., Kumar, N., & Kashyap, K. (2021). Mechanical and thermal properties of NaOH treated sisal natural fiber reinforced polymer composites: Barium sulphate used as filler. *Mater. Today: Proceedings 2021, 45,* 5575–5578 https://doi.org/10.1016/j.matpr.2021.02.310.

Kuwahara, Y., Liu, W., Makio, M., & Otsuka, K. (2016). In situ AFM study of crystal growth on a barite (001) surface in BaSO4 solutions at 30 OC. *Minerals, 6,* 117. https://doi.org/10.3390/min6040117.

Li, L., Yan, Z., He, X., Zhang, X., Wang, S., Guo, S., Tang, N., & Wang, X. (2021). A facile method to control the morphologies of barium sulfate particles by using carboxylic carbon quantum dots as a regulator. *Colloids Surf. A Physicochem. Eng., 631*, 127668. https://doi.org/10.1016/j.colsurfa.2021.127668

Liu, Y., Dai, Z., Kan, A. T., Tomson, M. B., & Zhang, P. (2022). Investigation of sorptive interaction between phosphonate inhibitor and barium sulfate for oilfield scale control. *J. Pet. Sci. Eng., 208,* 109425. https://doi.org/10.1016/j.petrol.2021.109425

Lopresti, M., Palin, L., Alberto, G., Cantamessa, S., & Milanesio, M. (2021). Epoxy resins composites for X-ray shielding materials additivated by coated barium sulfate with improved dispersibility. *Materials Today Communications, 26*, 101888. https://doi.org/10.1016/j.mtcomm.2020.101888.

Mhatre, S., Naik, S., & Patravale, V. (2021). Exploring green and industrially scalable microfluidizer™ technology for development of barium sulphate nanosuspension for enhanced contrasting. *J Drug Deliv. Sci. Technol., 64*, 102567 https://doi.org/10.1016/j.jddst.2021.102567

Mahieux, P. Y., Aubert, J. E., Cyr, M., Coutand, M., & Husson, B. (2010). Quantitative mineralogical composition of complex mineral wastes-contribution of the Rietveld method. *Waste Manage, 30,* 378-388. https://doi.org/10.1016/j.wasman.2009.10.023

Qasim, K. F., & Mousa, M. A. (2021). Electrical and dielectric properties of self-assembled polyaniline on barium sulphate surface. *Egypt. J. Pet., 30,* 9-19. https://doi.org/10.1016/j.ejpe.2021.09.001

Rodriguez-Carvajal, J. (2005). *Program Fullprof.2k, version 3.30.* Laboratoire Leon Brillouin, France.

Sadeghalvad, B., Khorshidi, N., Azadmehr, A., & Sillanpaa, M. (2021). Sorption, mechanism, and behavior of sulfate on various adsorbents: A critical review. *Chemosphere, 263*, 128064. https://doi.org/10.1016/j.chemosphere.2020.128064.

Shaw, S. S., Sorbie, K. S., & Boak, L. S. (2012). The effects of barium sulfate saturation ratio, calcium, and magnesium on the inhibition efficiency-part I: Phosphonate scale inhibitors. *SPE Prod & Oper., 27*(04), 390-403. https://doi.org/10.2118/130374-PA

Shikazono, N. (1994). Precipitation of barite in sulfate-sulfide deposits in back-arc basins. Geochim. Cosmochim. *Acta, 58,* 2203. https://doi.org/10.1016/0016-7037(94)90005-1

Smith, E., Hamilton-Taylor, J., Davison, W., Fullwood, N. J., & McGrath, M. (2004). The effect of humic substances on barite precipitation-dissolution behavior in natural and synthetic lake waters. *Chem. Geol., 207*, 81. https://doi.org/10.1016/j.chemgeo.2004.02.005

Turner, A., & Filella, M. (2021). Corrigendum to the influence of additives on the fate of plastics in the marine environment, exemplified with barium sulphate. *Mar. Pollut. Bull., 162*, 111787 https://doi.org/10.1016/j.marpolbul.2020.111352.

Widanagamage, I. H., Griffith, E. M., Singer, D. M., Scher, H. D., Buckley, W. P., & Senko, J. M. (2015). Controls on stable Sr-isotope fractionation in continental barite. *Chem. Geol., 2015*, 411. https://doi.org/10.1016/j.chemgeo.2015.07.011

Widanagamage, I. H., Schauble, E. A., Scher, H. D., & Griffith, E. M. (2014). Stable strontium isotope fractionation in synthetic barite. *Geochim. Cosmochim. Acta, 140*, 58. https://doi.org/10.1016/j.gca.2014.10.004

Widanagamage, I. H., Waldron, A. R., & Glamoclija, M. (2018). Controls on barite crystal morphology during abiotic precipitation. *Minerals, 8*, 480. https://doi.org/10.3390/min8110480

Wong, D. C. Y., Jaworski, Z., & Nienow, A. W. (2001). Effect of ion excess on particle size and morphology during barium sulfate precipitation: An experimental study. *Chem. Eng. Sci., 6*, 727. https://doi.org/10.1016/S0009-2509(00)00282-7

Isolation of Zn and Cr in Biosolid Waste by Extraction Process Using Sulfuric Acid

ORIGINALITY REPORT

11%	11%	0%	0%
SIMILARITY INDEX	INTERNET SOURCES	PUBLICATIONS	STUDENT PAPERS

PRIMARY SOURCES

1	www.mpdi.com Internet Source	11%

Exclude quotes	Off	Exclude matches	Off
Exclude bibliography	Off		